Eur. Phys. J. B **15**, 205–210 (2000)

THE EUROPEAN PHYSICAL JOURNAL B

EDP Sciences

Enhanced reactivity of domain walls in WO_3 with sodium

A. Aird[a] and E.K.H. Salje

Department of Earth Sciences and IRC in Superconductivity, University of Cambridge, Downing Street, Cambridge, CB2 3EQ, UK

Received 3 September 1999 and Received in final form 15 December 1999

Abstract. A possible new high temperature superconducting phase was recently reported in WO_3:Na. We have examined the reaction between sodium vapour and WO_3, and compared the phases formed by the reaction to previously known WO_3 phases. By using light microscopy and electron microprobe analysis, domain walls from the interior of the crystal are shown to have a much higher Na content than bulk material after reaction with Na vapour. This indicates preferential transport along the domain walls. The result is very similar to a reduction reaction of WO_3 crystals in which twin walls lose oxygen preferentially. Oxygen deficient twin walls are superconducting with $T_c \approx 3$ K.

PACS. 61.72.Mm Grain and twin boundaries – 66.30.-h Diffusion in solids – 81.70.Jb Chemical composition analysis, chemical depth and dopant profiling

1 Introduction

It has recently been reported by Reich and Tsabba [1] that sodium doped WO_3 shows a possible new phase with superconducting transition temperature of 91 K. If this is confirmed, it would be the first tungsten based high temperature superconductor. Low temperature superconductivity in Na_xWO_3 has been known for a long time [2–4], and sheet superconductivity in WO_{3-x} was recently found by Aird and Salje [5]. Our current research relates to the possibility of wall superconductivity in Na_xWO_3.

In this paper we discuss the phases found on reacting WO_3 with sodium vapour, and compare them to previously known WO_3, WO_{3-x} and Na_xWO_3 structures. We also find enhanced reactivity in domain walls of WO_3 compared with bulk material. This fast diffusion sets up the possibility of making solid state devices, and has been discussed before but never documented [6]. There has been little previous experimental evidence in other materials that domain walls enhance chemical reactivity compared with the bulk reactivity. The preferential sodium transport in twin walls described here in WO_3 by a gas transport reaction with sodium vapour is an exception to this.

The effect of the domain walls may be described as follows. From continuum elasticity theory, the equilibrium strain for a twin wall is found to be $e(x) = e_o \tanh(x/w)$. The high elastic energy of twin walls leads to a continuous but coherent lattice distortion. This can be contrasted with grain boundaries, where normally two crystals will fit together incoherently, leading to topological defects which can act as a sink for the diffusing atoms. Hence a previous difficulty in looking for domain wall reactivity was the higher reactivity of the grain boundaries. Here this problem is eliminated by using twinned single crystals. Twin walls can also offer paths of increased mobility for atomic particles. Locherer *et al.* [7] measured the orthorhombic-tetragonal domain wall thickness 2W in WO_3 to be c.a. 42 Å, using X-ray diffraction techniques.

Table 1. WO_3 phases.

Phase	Structure	Space group	Temp range	Refs.
ε-WO_3	monoclinic	Pc	Below 230 K	[21]
δ-WO_3	triclinic	$P\bar{1}$	230 K to 290 K	[20,21]
γ-WO_3	monoclinic	$P2_1/n$	290 K to 600 K	[19]
β-WO_3	orthorhombic	Pmnb	600 K to 1000 K	[17]
α_2-WO_3	tetragonal	P4/ncc	1 000 K to 1 170 K	[16,18]
α_1-WO_3	tetragonal	P4/nmm	above 1 170 K	[18]

Table 1 lists the six phases ($\alpha_1 - \varepsilon$) of stoichiometric WO_3, which occur over the temperature range 230 K to 970 K. These all have distorted perovskite type structures with the 12 fold coordinated "A" sites of the perovskite empty. At room temperature the monoclinic γ or triclinic δ phase is usually observed.

The domain wall orientations in WO_3 are perpendicular to the cleavage plane. At room temperature two sets of nearly orthogonal ferroelastic walls can be seen, oriented at 45 ° with respect to each other. The orientation of these walls corresponds to the ferroelastic transformation of the tetragonal-orthorhombic and orthorhombic-monoclinic transition in WO_3. Figure 1 shows an electron micrograph of these domain walls. In many samples only one wall orientation is observed, these parallel walls transverse the entire sample, *i.e.* the crystal has a "stripe"

[a] e-mail: aa224@esc.cam.ac.uk

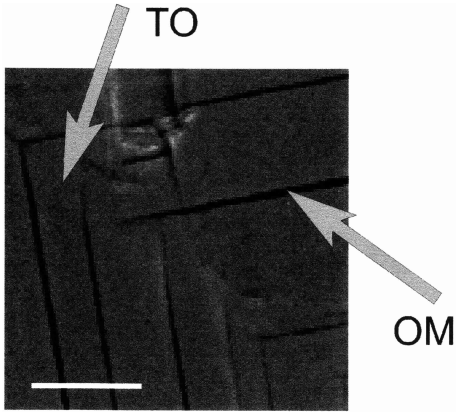

Fig. 1. Tetragonal-orthorhombic (TO) and orthorhombic-monoclinic (OM) domain walls in WO_3. The OM walls correspond to the dark lines shown in the SEM photograph and the TO walls divide regions of parallel OM walls. The scale bar is 100 μm.

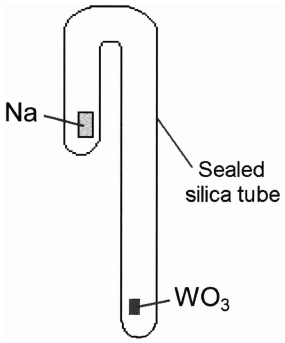

Fig. 2. The sodium vapour reaction was carried out in a sealed evacuated U-shape silica tube.

domain pattern. The domain structure of twinned WO_3 is easily seen by polarised light microscopy. The reaction with sodium results in a colour change, so that inspection with an optical microscope reveals reacted areas and their locations relative to the domain walls.

When WO_3 is chemically reduced to WO_{3-x}, either crystal structures with crystallographic shear planes or pentagonal tunnels are found [8,9] or a weakly reduced tetragonal structure (α_3) without such extended crystallographic defects occurs [10]. This tetragonal structure with space group $P\bar{4}2_1m$ has twice the unit cell volume of the unreduced tetragonal phase α_1. The lattice parameter transformation is $a \rightarrow \sqrt{2}a$ and $c \rightarrow c$. The lattice parameters are $a/\sqrt{2} = 0.522\,07$ nm and $c = 0.387\,81$ nm. This is smaller than the equivalent unit cells of both of the high temperature tetragonal phases α_1 and α_2. The α_1 phase has $a = 0.530\,31$ nm, $c = 0.393\,48$ nm, and the α_2 phase has $a = 0.528\,85$ nm, $c = 0.786\,26$ nm with cell doubling along the crystallographic c axis [19].

The reaction between WO_3 and sodium is as follows.

$$WO_3 + x\mathrm{Na} \rightarrow \mathrm{Na}_x\mathrm{WO}_3 \quad 0 \leq x \leq 1.$$

At very low values of x the Na_xWO_3 adopts low symmetry structures similar to undoped WO_3 [11]. At full saturation, *i.e.* at $x = 1$, a cubic structure is formed, with sodium occupying the perovskite A sites. At intermediate compositions, a non-stoichiometric sodium tungsten bronze, Na_xWO_3 is formed [12–15].

Two separate tetragonal phases of Na_xWO_3 are known in this intermediate range. The tetragonal II bronze (TII) has x up to 0.2 and is dark blue in colour. The TII phase has P4/nmm symmetry, the same as the high temperature α_1 phase, although the lattice parameters of $a = 0.524\,92$ nm and $c = 0.389\,53$ nm at $x = 0.1$ [14] are smaller than α_1. The tetragonal I bronze (TI) has blue colour, with $0.2 < x < 0.5$. The TI phase has $a = 1.209\,7$ nm; $c = 0.375\,4$ nm for $x = 0.33$ and $a = 1.215\,0$ nm; $c = 0.376\,9$ nm for $x = 0.48$ [15]. Shanks [2] has observed superconductivity in the tetragonal I phase with T_c of up to 3 K, dependent on composition. The transition from tetragonal (II) to (I) involves a rotation some of the square perovskite units from the ideal cubic structure, forming triangular and pentagonal tunnels *via* cylindrical rotation faults. The pentagonal and the original square tunnels fill with sodium, but the triangular tunnels are too small.

The purpose of this paper is to report on the identification of a novel Na-bearing phase which forms under reduction of WO_3 in the presence of Na vapour.

2 Experimental

WO_3 crystals were made by recrystallisation of WO_3 powder, by heating at 1 170 K for 100 hours to get rid of excess gas, then heating at 1 720 K for 2 hours followed by quenching [5,7]. Reaction with sodium was carried out by heating the triclinic WO_3 sample at 730 K for variable time lengths with metallic sodium. A U-shaped silica tube was used, in which the sample and the metallic sodium were placed in opposite ends (Fig. 2). The tube was evacuated and heated, so that sodium vapour was transported onto the sample. If the temperature gradient was set up such that the gas flow was favourable, the sodium would enter the WO_3 crystal. It was also possible to set up the gas flow so that the sodium would reduce the surface, forming Na_2O, and not entering the crystal itself. Parts of the sample further from the surface subsequently became reacted due to the high mobility of sodium in the WO_3, or in the case of reduced material, due to the oxygen mobility in WO_3. Three samples are examined in this paper, all reacted with sodium at 730 K. Sample A was reacted for 17 hours, sample B for 24 hours and sample C for 22 hours. The gas flow for these samples resulted in incorporation of sodium in each. However, due to small and uncontrollable differences in temperature gradient, larger differences in the amount of gas flow arose, and the reaction times are not directly proportional to the degree of reactivity. This had to be determined by subsequent chemical analysis.

Table 2. Na_xWO_3 structures.

Sodium content	Structure	Colour
Very low x	similar to WO_3 structures	Green/yellow
$x < 0.2$	tetragonal II structure also found just below $x = 0.2$	Dark blue
$0.2 < x < 0.5$	tetragonal I structure - superconducting	Blue
$x > 0.5$	cubic	Gradual change from red to bronze/yellow

Powder X-ray diffraction was used for qualitative phase analysis of the samples, with indexing of the reflections based on known possible crystal structures and their lattice parameters. Samples were crushed with an agate mortar and pestle in an air atmosphere. A monochromatic copper K-α_1 X-ray beam was used, along with an Inel CPS 120 detector. Silicon was used as an internal standard to calibrate the diffraction geometry.

Microanalysis of the crystals was carried out on a Cameca SX-50 electron microprobe. This was set up to measure the Na:K_α, W:M_α and O:K_α peaks. The SX-50 has 3 spectrometers, and to measure the three peaks the WDS detectors were set up with TAP, PET and PC1 crystals which have d-spacings of 25 Å, 8.5 Å and 60 Å respectively. The pulse height analyser minimum threshold was set to 0.3 V for each spectrometer and the counting to integral mode. Counting in integral mode means getting interference from the second order sodium Bragg peak in with the counts from the oxygen peak. This is estimated to cause a 2% error, which has been corrected for in the results. A NaCl standard was used for Na:K_α and a WO_3 standard was used for both tungsten and oxygen counts. The sodium chloride standard was stored in a dessicator to avoid incorporation of water, and was coated with a carbon layer 20 nm thick. The carbon resulted in a loss of X-ray intensity of around 3% in the standard at 10 kV. The sample results have been scaled to take account of this. Although sodium chloride may be susceptible to beam damage at high current densities, no visible effects occurred under the conditions used. A count time of 20 s was used for each element to be analysed, and a background measurement was subtracted from each peak.

For the microprobe analysis the reacted WO_3 samples were cleaved and mounted on an aluminium stub using a piece of sticky carbon film for electrical contact. As the WO_3 has a high electrical conductivity, it was not necessary to coat the samples with a conducting material. The sample was viewed in reflected light in order to locate the areas with reacted domain boundaries, and to monitor surface quality. The electron beam was focussed and the HV was set to 10 kV. Based on the beam width, this was estimated to give a spatial resolution of approx. 1–2 microns. The beam current was set to 50 nA. Several linescans of the W, Na and O content were measured across the domain boundaries. For each measurement, peak intensities were used to calculate standard deviations in the concentration of the three elements.

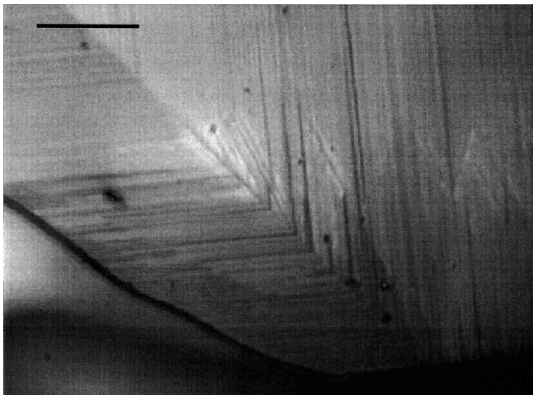

Fig. 3. Reacted monoclinic-orthorhombic boundaries. The scale bar is 50 μm.

3 Results

For inclusion of sodium, the reacted material firstly turns to a bluish-black coloured product which is distinct from the yellow-green of the starting material. This was seen in polarised light to consist of domains in the same positions as the unreacted WO_3 domains, but with a blue or orange colour depending on orientation. The next stage was a transformation to a red colour, and finally a bronze colour. Table 2 outlines various phases which have been found in Na_xWO_3 as a function of the sodium content.

During the early part of the reaction, the monoclinic-orthorhombic domain walls react most readily, while the bulk remains unreacted, as shown in Figure 3. The areas most reacted in this sample are near to the edge of the crystal or to an orthorhombic-tetragonal domain wall. This shows that fast diffusion occurs along this wall. In addition, as a secondary effect, the additional sodium quickly diffuses outwards into the monoclinic-orthorhombic domain walls. It is unclear why the monoclinic-orthorhombic walls have reacted, since the nominal reaction temperature of 730 K is above the monoclinic to orthorhombic transition temperature of 600 K. A possibility is that this reaction occurs after the annealing at 730 K, during the cooling process.

At a later stage of reaction, the reflected light microscope image showed that the regions along the original orthorhombic-tetragonal twin walls were more highly reacted. This was seen directly *via* the colour change in a cleaved sample. In Figure 4a, a sample with several domain walls is shown. Increased levels of sodium cause the crystal to change colour to red, in contrast with the blue

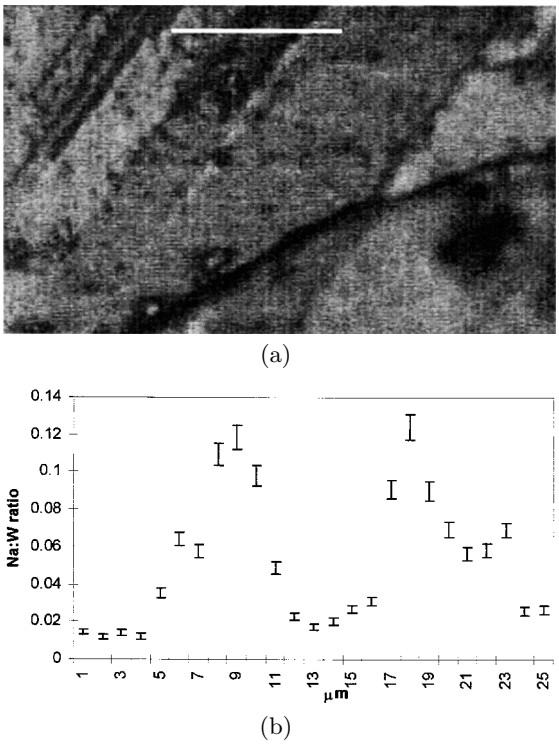

Fig. 4. (a) Cleaved crystal with orthorhombic-tetragonal walls reacted. The white line (of length 25 μm) corresponds to the position of the microprobe linescan shown in Figure 4b. (b) Microprobe linescan showing measured Na:W atom ratios at 1 μm steps.

and orange domains in the bulk. This occurs towards the edge of the crystal, and along the twin walls.

The O:W and Na:W ratios were measured by electron microprobe in a linescan along the marked region in Figure 4a. The O:W ratios were found to be very close to the stoichiometric value of 3, with variations of c.a. 4% which is too small to be significant against error levels. The Na:W ratio on the other hand shows approximately a 400% variation, with huge maxima at the domain wall positions. This is shown in Figure 4b. It can clearly be seen from Figure 4a that the locations of the twin walls are at 8 μm, 19 μm and 22 μm from the start point of the scan. At these walls, the sodium to tungsten atom ratio, Na:W, is around 0.13. This is equivalent to a sodium content of $Na_{0.13}WO_3$. In the surrounding bulk the Na:W ratio drops off to 0.03.

The wall region, with a Na:W ratio of 0.13, has changed to reddish colour. The value of $x = 0.13$ corresponds to the composition range expected for the TII sodium phase, although the colour change is then more extreme than expected. It is likely that the measured composition is slightly low due to spatial averaging over the less reacted surrounding areas during the microprobe measurements.

The accuracy of the probe measurements is dependent on many factors. Firstly, there is a statistical counting error, which has approximately a Gaussian distribution. This has been estimated as $\sqrt{N}$, where N is the total number of counts for each measurement. Inter-element absorption factors are taken into account by the ZAF analysis carried out by the Link "Spectra" microprobe software.

Another factor in the accuracy of microprobe analysis is surface quality and alignment. We have selected areas of surface to analyse by inspection of quality with a reflected light microscope. However, surface quality may be a source of error particularly around the domain boundaries, due to the surface not being completely flat and due to more reacted areas having higher surface roughness in comparison with the standards. The 4% oxygen variation may well arise from this, and the error bars in the sodium measurements also take into account a 4% variation due to surface roughness. It is also possible to get some sodium evaporation in the beam – however, repeated measurements of the same points on the crystal surface yielded no significant difference in sodium content. Hence this effect appears to be insignificant.

These factors all affect the microprobe results, but this is important for exact numerical values rather than for semi-quantitative comparison of sodium content throughout the structure, which clearly shows large maxima in the domain boundaries.

Figure 5 shows the X-ray powder diffraction spectra of sample A (shown in Fig. 4a) and of the two other samples, B and C.

4 Discussion

We have shown that there is a much higher concentration of sodium in the domain walls. We now examine the phases found by XRD in the reacted crystal, and attempt to match them to known phases.

The following tetragonal phases are now considered. Firstly, there are the two high temperature stoichiometric WO_3 phases α_1 and α_2 [16–18]. There is also the reduced (WO_{3-x}) phase α_3, as described by Aird *et al.* [10], and the two tetragonal phases TI and TII of Na_xWO_3 [14,15]. The powder spectra of these phases were compared, and it was found that the α_1 and α_2 phases are similar to both the reduced α_3 phase and the TII bronze, although with different lattice parameters. Details of the lattice parameters are given in Table 3. The powder spectrum of the TI phase is quite different.

The X-ray powder diffraction spectra of samples A, B and C (Fig. 5) can be compared with the spectra for the triclinic δ phase and the tetragonal tungsten oxide phases. It is clear that the bulk of the material in sample A is triclinic. There also appears to be a small amount of tetragonal phase present. Samples B and C likewise contain a phase mixture of tetragonal and triclinic, with mainly the tetragonal phase in sample C.

X-ray diffraction traces were re-measured after a couple of days and it was found that the amount of tetragonal material decreased while the amount of triclinic material increased, *i.e.* that the powdered sample re-oxidised in air. This is very similar to the behaviour observed in oxygen

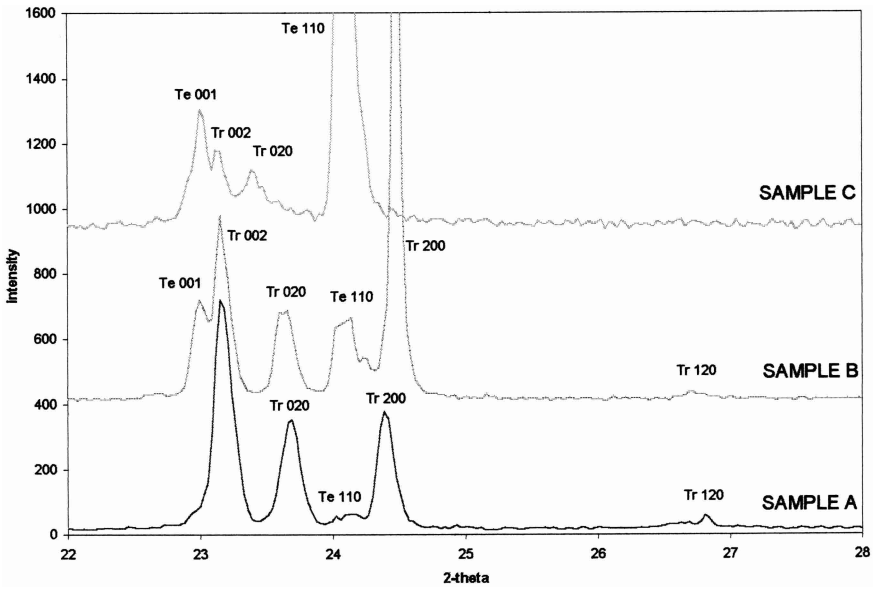

Fig. 5. Powder X-ray diffraction spectra from three different samples containing sodium. All three samples are a mixture of tetragonal (Te) and triclinic (Tr) material.

Table 3. Structures of various tetragonal phases.

phase	chemistry	Space group	a (nm) (using α_2 unit cell axes)	c (nm) (using α_2 unit cell axes)	a/c ratio
α_1	WO_3	P4/ncc	0.528 85	0.393 13	1.345 2
α_2	WO_3	P4/nmm	0.530 31	0.393 48	1.347 7
TII	$Na_{0.1}WO_3$	P4/nmm	0.524 92	0.389 53	1.347 6
α_3	WO_{3-x}	$P\bar{4}2_1m$	0.522 07	0.387 81	1.346 2
Sample C	Na:WO_3		0.521 31	0.387 30	1.346 0

deficient samples with no sodium [10]. Hence the microprobe measurements of an O:W ratio of 3 may be due to re-oxidation on the surface layer. Tetragonal material in the interior of similar crystals is stable in air over a time period of at least several months.

We know that the bulk of the material in sample A has a Na:W ratio of 0.03, and that most of the crystal is triclinic. This suggests that the bulk consists of slightly sodium enhanced δ phase. The tetragonal phase corresponds to the most reduced parts of the crystal. It is possible that in the case of oxygen, as with sodium, these most reacted parts correspond to the domain walls, although surface re-oxidation prevents testing this by microprobe measurements. We now try to identify which particular tetragonal phase is present.

Sample C contains the largest proportion of the tetragonal phase also found in samples A and B. The XRD peaks of sample C have been indexed, and the lattice parameters found, using least squares refinement of 9 reflections, to be $a = 0.521\,31$ nm and $c = 0.387\,30$ nm with standard deviations of 0.000 39 nm in a and 0.000 25 nm in c. The lattice parameters are smaller than those of the other tetragonal phases but they almost co-incide with the reduced α_3 phase.

In consideration of which tetragonal phase is actually present in the Na:WO_3, the a/c ratios were calculated for each phase and listed in Table 3. Phase TI is not included as it had a very different XRD powder spectrum. Although all phases had a very similar value of close to 1.346 with only a 0.2% difference between largest and smallest, the a/c ratio found for sample C was closest to that of the reduced material α_3. The standard deviation in this value is 1.33×10^{-3}. This, along with the fact that the lattice parameters are also closest to the α_3 values suggests that part of the sample has a structure like that of α_3.

In summary, the microprobe results clearly show that there is a higher concentration of sodium in the domain walls. The high sodium content is due to the higher sodium mobility in the walls. The sodium comes in from outside and moves firstly along the walls, then through the bulk.

A triclinic and a tetragonal phase have been found, but no other phases have been observed. The bulk of the crystal is triclinic, and would appear to be slightly sodium enhanced δ phase. The tetragonal phase corresponds to the most highly reduced parts of the bulk interior. Like the sodium, these may be the domain walls, in which case we also have a Na enriched tetragonal phase, similar to α_3. The Na bearing material then must transform during the doping process from the δ phase into the α_3 phase. Alternatively, the Na along the domain walls may be in a different phase altogether, which is not present in

large enough volumes to be detectable by X-ray diffraction.

We are grateful to Stephen Reed of Department of Earth Sciences, Cambridge University for experimental assistance and helpful discussion.

References

1. S. Reich, Y. Tsabba, Eur. Phys. J. B **9**, 1 (1999).
2. H.R. Shanks, Solid State Commun. **15**, 753 (1974).
3. I.A. Garifullin, N.N. Garif'yanov, V.Yu Maramzin, G.G. Khaliullin, Solid State Commun. **85**, 1001 (1993).
4. N.N. Garif'yanov, S.Ya Khlebnikov, I.S. Khlebnikov, I.A. Garifullin, Czech. J. Phys. **46**, S2, 855 (1996).
5. A. Aird, E.K.H. Salje, J. Phys. Cond. Matter **10**, 377 (1998).
6. J. Maier, *Interfaces* in *Oxygen Ion and Mixed Conductors and their Technological Applications*, edited by H.L. Tuller, J. Schoonman, I. Riess (Kluwer Academic Publishers, Dordrecht, 2000).
7. K.R. Locherer, J. Chrosch, E.K.H. Salje, Phase Transit. **67**, 51 (1998).
8. T. Ekström, E. Salje, R.J.D. Tilley, J. Solid State Chem. **40**, 75 (1981).
9. M. Sundberg, J. Sol. State Chem. **35**, 120 (1980).
10. A. Aird, M.C. Domeneghetti, F. Mazzi, V. Tazzoli, E.K.H. Salje, J. Phys. Cond. Matter **10**, L569 (1998).
11. E. Salje, Ferroelectrics **12**, 215 (1976).
12. R. Clarke, Phys. Rev. Lett **39**, 1550 (1977).
13. M. Sato, B.H. Grier, G. Shirane, T. Akahane, Phys. Rev. B **25**, 6876 (1982).
14. S.T. Triantafyllou, P.C. Christidis, Ch.B. Lioutas, J. Solid State Chem. **133**, 479 (1997).
15. F. Takusagawa, R.A. Jacobson, J. Solid State Chem. **18**, 163 (1976).
16. W.L. Kehl, R.G. Hay, D. Wahl, J. Appl. Phys. **23**, 212 (1952).
17. E. Salje, Acta Cryst. B **33**, 574 (1977).
18. K.R. Locherer, I.P. Swainson, E.K.H. Salje, J. Phys. Cond. Matter **11**, 4143 (1999).
19. P.M. Woodward, A.W. Sleight, J. Sol. State Chem. **131**, 9 (1997).
20. R. Diehl, G. Brandt, E. Salje, Acta Cryst. B **24**, 1105 (1978).
21. E. Salje, S. Rehmann, F. Pobell, D. Morris, K.S. Knight, T. Herrmannsdörfer, M.T. Dove, J. Phys. Cond. Matter **9**, 6563 (1997).